Spin picture of the one-dimensional Hubbard model: Two-fluid structure and phase dynamics

Spin picture of the one-dimensional Hubbard model: Two-fluid structure and phase dynamics

Arianna Montorsi and Vittorio Penna
Dipartimento di Fisica and Unità INFM, Politecnico di Torino, I-10129 Torino, Italy
(Received 12 May 1999)

We propose a scheme for investigating the quantum dynamics of interacting electron models by means of a time-dependent variational principle and spin coherent states of space lattice operators. We apply such a scheme to the one-dimensional Hubbard model, and solve the resulting equations in different regimes. In particular, we find that at low densities the dynamics is mapped into two coupled nonlinear Schrödinger equations, whereas near half-filling the model is described by two coupled Josephson-junction arrays. Focusing then to the case in which only the phases of the spin variables are dynamically active, we examine a number of different solutions corresponding to the excitations of few macroscopic modes. Based on fixed-point equations of the simpler among them, we show that the standard one-band ground-state phase space is found. [S0163-1829(99)01441-1]

I. INTRODUCTION

Investigating quantum dynamics of strongly correlated many-body systems is a hard task since, even for extremely simplified models, the interactions of the large number of degrees of freedom are usually affected by a nonlinear character. At the operational level this entails the impossibility of evaluating explicitly the action of the propagator known from the Schrödinger equation, that is the evolution $|\Phi\rangle = \exp[-itH/\hbar]|\Phi_0\rangle$ of a state $|\Phi_0\rangle$ governed by the Hamiltonian H. A standard way to reduce such a difficulty to a more tractable form consists in recasting the purely quantum problem within an appropriate coherent states picture once the algebraic structure characterizing H has been identified. This leads to represent the system evolution through the equations of motion issued from an effective classical Hamiltonian $\mathcal{H}$ expressed in terms of the coherent-state parameters.[1]

A systematic development of such an approach is provided by the time-dependent variational principle (TDVP) procedure.[2] This amounts to constructing a trial macroscopic wave function $|\Psi\rangle$ that contains time-dependent parameters whose evolution is derived so as to optimize the approximation of the quantum propagator action.[3] On this basis, using the generalized coherent states to construct the trial state $|\Psi\rangle$ is quite advantageous in that the coherent-state parameters naturally label $|\Psi\rangle$ and make explicit its dependence on the algebraic structure of H, namely, on the operators describing the microscopic physical processes therein. By making the phase that appears in $|\Psi\rangle$ coincide with the effective action, the Schrödinger equation turns out to be automatically satisfied when projected onto $|\Psi\rangle$.

In a recent paper[4] such a scheme was specialized to the case of interacting electrons described by the Hubbard Hamiltonian. There the coherent states entering $|\Psi\rangle$ were specific to the physical regimes (e.g., superconducting, antiferromagnetic, etc.), the latter selecting case by case the appropriate approximate algebraic framework within the Hamiltonian dynamical algebra.

The standpoint here adopted is instead to implement a unified TDVP treatment independent of the particular physical regime and provide a coherent state picture of electrons on the ambient lattice, whatever the model interaction actually is. Even though this approach is quite general, in the sequel we shall develop it for the Hubbard Hamiltonian.

It is well known that the Hubbard Hamiltonian can be rewritten in terms of two coupled XX models of 1/2 spin operators by means of the Jordan-Wigner transformation. Such a transformation can be performed in any dimension as well as, in principle, for any electron Hamiltonian, and leads quite naturally to a picture relying on spin coherent states (SCS).[1] When this is used explicitly within the TDVP framework, the resulting equations of motion are recognized to describe two coupled fluids, which dynamics we shall discuss.

A basic trait of the spin description is that its semiclassical version is more reliable the more the spins are large.[5] Since this feature is in general not realized when starting from quantum 1/2 spin operators, we shall look here, in particular, for solutions of the equations of motions corresponding to the macroscopic excitations of few system modes, in which case we expect to describe actual regimes for the Hubbard model itself. The problem of mode requantization, naturally in order due to the expected quantum character of the low-temperature regime, is left to a successive analysis.[6]

The choice of $|\Psi\rangle$ as a direct product of single-site Bloch states, representing the only assumption for our construction, deserves some comments as to the expected reduction of the number of states in the Hilbert space that are actually available for the system dynamics. Such an effect usually occurs in a number of mean-field approximations like the standard Hartree-Fock (HF) in which the dominating features of the system are accounted for in an explicit way thanks to an extreme reduction of the states accessible to the system.

In this respect, using coherent states relative to the operators of H defined in the ambient lattice is by construction less restrictive than using a subset of states tailored for a specific regime. The advantage coming from this choice is manifold. First, the structure of $|\Psi\rangle$ is however able to produce an effective Hamiltonian $\mathcal{H}$ that inherits both the nonlocal and the nonlinear character of H, contrary to the Hartree-Fock (HF) scheme, in which H reduces to a sum of single-site linear Hamiltonians. In passing, we notice that in many cases $\mathcal{H}$ exhibits a form that is endowed with the same complexity

of H. In fact, the nontrivial form of $\mathcal{H}$ reflects the basic character of the TDVP method that singles out $|\Psi\rangle$ variationally as the best solution to the original Schrödinger equation[3], whereas within the HF approximation what is solved is a different Schrödinger equation, involving just the linearized Hamiltonian.

Second, as a consequence of the above feature, also the propagation of any initial state is sustained by the full Hamiltonian, rather than by its linearized HF version. Indeed, it is easily shown that the latter entails quantum states whose time evolution is periodic, while the TDVP dynamics is endowed with a much richer structure. In particular, the dynamics of the expectation values of spin operators (our dynamical variables) is consistently reproduced, whereas, when turning to expectation values of products of spin operators, the description obtained does not differ substantially from the one that can be achieved within the random-phase approximation.

The Jordan-Wigner transformation mentioned above amounts to rewriting the electron annihilation operators $c_{j,\eta}$, with $\eta=\uparrow,\downarrow$, in terms of Pauli spin matrices $\sigma_{a,j},\tau_{a,j}$, with $a=1,2,3$, which locally form two (commuting) $su(2)$ algebras. For the Hubbard model, it turns out that in dimension $D>1$ the possible transformed Hamiltonians differ from each other due to a certain exponential factor in front of the hopping term, which form in fact depends on the ordering chosen for labeling the lattice sites. This problem has been already investigated in the literature,[6] and in the present paper we shall limit our discussion to the one-dimensional (1D) case. Explicitly,

$$c_{j,\uparrow}=P_j(\sigma_3)\sigma_j^-\ ,\ \ c_{j,\downarrow}=P_L(\sigma_3)P_j(\tau_3)\ \tau_j^-\ , \tag{1}$$

where $P_j(\nu_3)\doteq\Pi_{\ell<j}\,\sigma_{3,\ell}$, $\nu=\sigma,\tau$, from which the expressions for $c^\dagger_{\mathbf{j},\sigma}$ are straightforwardly derived. Here L is the number of lattice sites, $\nu_j^+\doteq\nu_{1,j}+i\,\nu_{2,j}$, with $\nu=\sigma,\tau$. Remarkably, this transformation maps fermions, which anticommute on different sites, into spins, which commute on different sites, i.e., $[\sigma_{a,j},\sigma_{b,\ell}]=0$ for $\ell\neq j$.

Once Eqs. (1) are inserted into the Hubbard Hamiltonian, the latter becomes

$$H=\sum_{j=1}^{L}\,[U\sigma_{3,j}\,\tau_{3,j}-T(\sigma_j^+\sigma_{j+1}^-+\tau_j^+\tau_{j+1}^-+\text{H.c.})], \tag{2}$$

when periodic boundary conditions are considered, and an odd number of holes N_η^h $(\eta=\uparrow,\downarrow)$ on both σ sublattices is assumed,[7] otherwise boundary terms (corresponding to $j=L$) in the hopping contribution depending on T have to be rewritten as $(e^{\pi(1-N_\uparrow^h)}\sigma_L^+\sigma_1^-+e^{\pi(1-N_\downarrow^h)}\tau_L^+\tau_1^-+\text{H.c.})$. In Eq. (2) the extra terms that take advantage of conserved quantities such as the total electron number and the magnetization have been ignored.

In the next section, based on the spin-coherent-state picture, we shall implement the TDVP procedure whereby one can derive from Eq. (2) the effective Hamiltonian and the related motion equations. In Sec. III, upon recognizing the two-fluid structure of the resulting model, we shall solve explicitly the motion equations of each fluid within a phase-locking approximation, and evidenciate how the Coulomb interaction drives the system to a transition (apparently related to the metal-insulator one) in which also the phases of the two fluids become strongly locked. Tunneling phenomena between the two fluids are also discussed. In Sec. IV we specialize to the study of solutions exhibiting a pure phase dynamics, and stress the aspect concerning the macroscopicity of the excited degrees of freedom. In Sec. V we show that the ground-state phase space known from standard mean-field treatments can be obtained within our scheme by analyzing the fixed points of a very simple collective phase solution, corresponding, in fact, to describe the whole lattice as a sum of two-site clusters. Finally Sec. VI is devoted to give some conclusions.

II. COHERENT-STATES PICTURE

Approaching interacting spin systems within a semiclassical limit has been deeply investigated. In particular, it is well understood that a consistent description can be obtained[1] by projecting the Hamiltonian onto a basis of SCS. In this case, an exact result obtained by Lieb[5] shows that the projected Hamiltonian reproduces the behavior of the original one the more the spins are large, and in any case it gives upper and lower bounds to the ground-state energy of the quantum Hamiltonian (the exact value being recovered for infinitely large spins). One-half SCS are given by

$$|\,\eta\rangle\equiv C(\,\eta)e^{\eta J_+}|-1/2\rangle, \tag{3}$$

where the maximum weight vector $|-1/2\rangle$ belongs to the J_3 spectrum $[J_3|\pm1/2\rangle=(\pm1/2)|\pm1/2\rangle]$ and fulfills the condition $J_-|0\rangle=0$, J_- $[J_+=(J_-)^+]$ representing the lowering (raising) operator. Also, defining the normalization factor as $C(\,\eta)=1/\sqrt{1+|\,\eta|^2}$ ensures the condition $\langle\,\eta|\,\eta\rangle=1$. The expectation values of generators $J_3,J_\pm$,

$$S_3=\langle J_3\rangle=\frac{|\,\eta|^2-1}{2(1+|\,\eta|^2)} \tag{4}$$

$$S_-=\langle J_-\rangle=\frac{\eta}{(1+|\,\eta|^2)}, \tag{5}$$

obtained by means of definition (3) $(\langle\bullet\rangle\doteq\langle\,\eta|\bullet|\,\eta\rangle)$, clearly exhibit their semiclassical character when considering the fact that S_3, $S_\pm$ satisfy the equation $S_3^2+S_2^2+S_1^2=1/4$ $[(S_+\doteq S_1+iS_2)]$, namely, the same sphere equation fulfilled by the classic counterpart of the spin (J_1,J_2,J_3) $(J_+\doteq J_1+iJ_2)$. In passing we notice that the spin variables, assuming limited values, keep track of the fermionic nature of the underlying system.

The set-up just developed can be readily extended to the interacting spins of H. Assigning at each site a pair of SCS $|\alpha_j\rangle$, $|\beta_j\rangle$ relative to the above σ-spin and τ-spin, respectively, allows one to implement the TDVP procedure that is essentially based on constructing a macroscopic trial wave function accounting for the microscopic processes of the system. The simplest choice for a spin model is realized through the state

$$|\Psi\rangle\equiv e^{iS/\hbar}|\alpha\rangle\otimes|\beta\rangle, \tag{6}$$

where $|\alpha\rangle\otimes|\beta\rangle=\otimes_j(|\alpha_j\rangle\otimes|\beta_j\rangle)$, that provides the expectation values $A_j^*=\langle\Psi|\sigma_j^+|\Psi\rangle$ $(B_j^*=\langle\Psi|\tau_j^+|\Psi\rangle)$ and A_{3j}

$=\langle\Psi|\sigma_{3,j}|\Psi\rangle$ ($B_{3j}=\langle\Psi|\tau_{3,j}|\Psi\rangle$) of σ spins (τ spins). The description of the microscopic dynamical activity in terms of such semiclassical variables (actually they correspond to an ensemble of classical spins) is achieved by showing that they obey a set of Hamiltonian equations standardly derived from imposing $|\Psi\rangle$ to obey the weaker version of the Schrödinger equation $\langle\Psi|(i\hbar\partial_t - H)|\Psi\rangle = 0$, the latter requirement leading as well to interpret S in Eq. (6) as the effective action. The explicit form of TDVP Hamiltonian generating such Hamiltonian equations turns out to be

$$\langle H\rangle = \langle\beta|\otimes\langle\alpha|H|\alpha\rangle\otimes|\beta\rangle,$$

while the Poisson brackets obeyed by the spin ensemble variables implicitly follow from the equations of motion themselves.

Hubbard Hamiltonian (2) in one dimension, when projected onto the trial state $|\alpha\rangle\otimes|\beta\rangle$, becomes

$$\langle H\rangle = N_s\frac{U}{4} + \frac{U}{2}(A_3+B_3) + U\sum_j A_{3j}B_{3j} + \mathcal{H}_T, \quad (7)$$

where $A_3 \doteq \Sigma_j A_{3j}$, $B_3 \doteq \Sigma_j B_{3j}$ and the hopping term $\mathcal{H}_T$, which reads

$$\mathcal{H}_T \doteq -T\sum_j (A_j^* A_{j+1} + B_j^* B_{j+1} + \text{H.c.}),$$

is nothing but the sum of two classical XX models. The Hamiltonian equations generated by the TDVP procedure are given by

$$i\dot{A}_j = (-\delta_A + UB_{3j})A_j + 2TA_{3j}(A_{j_+1} + A_{j-1}), \quad (8)$$

$$i\dot{B}_j = (-\delta_B + UA_{3j})B_j + 2TB_{3j}(B_{j_+1} + B_{j-1}), \quad (9)$$

$$i\dot{A}_{3j} = -T[A_j^*(A_{j_+1}+A_{j-1}) - A_j(A_{j_+1}^* + A_{j-1}^*)], \quad (10)$$

$$i\dot{B}_{3j} = -T[B_j^*(B_{j_+1}+B_{j-1}) - B_j(B_{j_+1}^* + B_{j-1}^*)], \quad (11)$$

where $\delta_A \doteq \mu_A - U/2$, $\delta_B \doteq \mu_B - U/2$, once the Hamiltonian $\langle H\rangle$ is rewritten in the form

$$\mathcal{H} \doteq \langle H\rangle + \mu_A\chi_A + \mu_B\chi_B \quad (12)$$

containing the constraints $\chi_A \doteq \sigma_A - A_3$, $\chi_B \doteq \sigma_B - B_3$ with Lagrange multipliers μ_A, μ_B. The Poisson brackets implicitly entailed by Eqs. (8)–(11) are given by

$$\{C_j^*, C_j\} = 2C_{3j}/i\hbar, \{C_{3j}, C_j^*\} = C_j^*/i\hbar$$

with $C = A, B$, and exhibit the structure of a (classical) angular momentum algebra. Also, they state that A_3, B_3, related to the total number of spin-up and spin-down electrons by the formulas

$$\left\langle \sum_j n_{j\uparrow}\right\rangle = A_3 + N_s/2, \quad \left\langle \sum_j n_{j\downarrow}\right\rangle = B_3 + N_s/2,$$

respectively, where $n_{j\sigma} = c_{j\sigma}^+ c_{j\sigma}$ ($\sigma = \uparrow, \downarrow$) are constants of motion since $\{A_3, \mathcal{H}\} = 0 = \{B_3, \mathcal{H}\}$. It is thus natural investigating spin dynamics when A_3, B_3 are assumed to have fixed values ν_A, ν_B by inserting such information via the constraints $\chi_A = 0 = \chi_B$.

The conservation, for each j, of the Casimir functions $C_{Aj} = A_{3j}^2 + |A_j|^2$ and $C_{Bj} = B_{3j}^2 + |B_j|^2$ is preserved as well. On the contrary, the total magnetization vector $\mathbf{M} = (M_x, M_y, M_z) = \Sigma_j \mathbf{M}_j$ (where $M_x + iM_y \doteq M^+$ with $M^+ = \Sigma_j \langle\Psi|\sigma_j^+\tau_j^-|\Psi\rangle = \Sigma_j A_j^* B_j$) is no longer conserved but only its z component $M_z = \frac{1}{2}\Sigma_j\langle\Psi|(\sigma_{3,j} - \tau_{3,j})|\Psi\rangle = \frac{1}{2}\Sigma_j(A_{3j} - B_{3j})$. In addition, we also notice that the usual particle-hole symmetry of the quantum Hamiltonian survives at the semiclassical level, and it is implemented by the particle-hole transformation $A_{3j} \to -A_{3j}$ and $B_{3j} \to -B_{3j}$.

Two remarks are now in order. First, due to the choice of macroscopic wave function (6), Hamiltonian (7), and Eqs. (8)–(11) mantain the same structure of Hamiltonian (2) and of the ensuing Heisenberg equations for the quantum spin variables, respectively, which feature is nontrivial.[4]

Moreover, we notice that, when moving from the lattice description to the continuum limit[8] ($C_j \to C(x) = |C(x)|e^{i\theta(x)}$, $x \in \mathbf{R}$, $C = A, B$), the resulting equations can be interpreted as two nonlinear Schrödinger equations (NLSE) for the order-parameter fields $A(x)$, $B(x)$. A part from the nonlinearity issued from $C_{3j} = \pm\sqrt{1/4 - |C_j|^2}$ that is capable of producing the standard quartic term $|C_j|^4$ for $|C_j|^2 \ll 1/4$, a further contribution in this sense comes from the Coulomb terms $UA_{3j}B_{3j}$. The standard reduction of the nonlinear Schrödinger equation to the continuity and the Bernoulli equation[9] governing the dynamics of the densitylike field $|C(x)|^2$ and the phase field $\theta(x)$, respectively, suggests that Eqs. (8)–(11) can be seen as describing the dynamics of a coupled two-fluid lattice model.

III. TWO-FLUID DYNAMICS

The two-fluid structure of Eqs. (8)–(9) has been recognized by reducing them to the standard form (cubic NLSE) thanks to the assumption $|C_j|^2 \ll 1/4$, namely, considering low-density fluids. In this regime the usual hydrodynamic picture is made far more complicated by the presence of A_{3j}, B_{3j} in front of the off-site T terms in Eq. (8), and Eq. (9). In fact such factors, in addition to the usual Laplacian-like terms of the (lattice) Schrödinger equation characterized by $A_{3j}, B_{3j} \simeq -1/2$, allow for the occurrence of configurations where the T terms exhibit anomalous signs ($A_{3j}, B_{3j} > 0$) through extended regions of the lattice. The investigations of the corresponding dynamics is deferred to a future study.

A regime exhibiting, in a sense, an opposite character ($|C_j|^2 \simeq 1/4 \to C_{3j} \simeq 0$) will be examined in the present section. The two-fluid structure still characterizes the motion equations even if the dynamics mainly concerns the phase variables, the densitylike variables $|C_j|^2$ being now essentially constant. It is worth noting as well how such a regime (characterized by a Bernoulli-like dynamics) is nothing but that the quantum phase regime naturally emerging from the XX model form of $\mathcal{H}_T$ for $|C_j| = \text{const}$. In fact, by setting first

$$A_j = R_j\exp(i\alpha_j), \quad B_j = S_j\exp(i\beta_j), \quad (13)$$

where $R_j^2 \equiv 1/4 - A_{3j}^2$, $S_j^2 \equiv 1/4 - B_{3j}^2$, consistently equipped with the standard canonical commutation relations

$\{\alpha_\ell, A_{3j}\} = \delta_{\ell,j}/i\hbar = \{\beta_\ell, B_{3j}\}$, and recasting then Eqs. (8)–(11) in the action-angle variable version contained in the Appendix, one is able to work out the two linear second-order equations,

$$\ddot{\alpha}_j = 4T^2[w(\beta_{j+1} - 2\beta_j + \beta_{j-1}) + (\alpha_{j+1} - 2\alpha_j + \alpha_{j-1})], \tag{14}$$

$$\ddot{\beta}_j = 4T^2[w(\alpha_{j+1} - 2\alpha_j + \alpha_{j-1}) + (\beta_{j+1} - 2\beta_j + \beta_{j-1})], \tag{15}$$

with $w = U/4T$, under the assumptions $|A_{3j}|, |B_{3j}| \ll 1/2$, $(\alpha_{j+1} - \alpha_j) \approx 0 \approx (\beta_{j+1} - \beta_j)$. Eqs. (14) and (15) describe dynamics of first-order quantities and exhibit the Lagrangian structure typical of two classical planar XX models nontrivially phase coupled for any nonvanishing $U \neq 0$.

Remarkably Eqs. (14) and (15) can be decoupled (and solved) upon defining $\theta_j = \alpha_j + \beta_j$, $\varphi_j = \alpha_j - \beta_j$. In this case they become

$$\ddot{\theta}_j = 4T^2(1+w)(\theta_{j+1} - 2\theta_j + \theta_{j-1}),$$

$$\ddot{\varphi}_j = 4T^2(1-w)(\varphi_{j+1} - 2\varphi_j + \varphi_{j-1}), \tag{16}$$

whose solution can be easily worked out in terms of Fourier modes. In particular, let us notice that the parameter w plays a relevant role, in that it drives the φ dynamics of the system from an oscillatory regime ($w < 1$) to a damped one ($w > 1$), whereas the θ dynamics remains purely oscillatory. This is explicit when considering any single mode solution of the form $\varphi_j(t;q) = \cos(\lambda_q t + \nu_j)$ and the ensuing dispersion relation

$$\lambda_q^2 = 16T^2(1-w)\sin^2(\pi q/L). \tag{17}$$

In terms of the original phases α_j and β_j this implies a phase-locking phenomenon for $w > 1$ ($U > 4T$), which is physically quite natural the more the on-site Coulomb repulsion becomes large. Having in mind the metal-insulator transition typical of the Hubbard model, which takes place at analogous values of U, we can argue that the change in the dynamical behavior parametrized by w might bear memory of such transition.

It is worth noting that, again to the first order, Eqs. (10) and (11) for A_{3j}, B_{3j} reduce to

$$\dot{A}_{3j} = -(T/2)(\alpha_{j+1} - 2\alpha_j + \alpha_{j-1}), \tag{18}$$

$$\dot{B}_{3j} = -(T/2)(\beta_{j+1} - 2\beta_j + \beta_{j-1}), \tag{19}$$

which, despite the approximation introduced, still shows a nontrivial time dependence of A_{3j}, B_{3j}. The comparison of the above equations with those describing the tunneling phenomena of Josephson junctions[11] is quite natural, coming from the fact the same equations can be obtained, in the same linearized form, when considering the Josephson-junction array Hamiltonian that can be represented in the simplified form by $H_{JJ} = \Sigma_j C_{3j}^2 - g\Sigma_j \cos(\gamma_{j+1} - \gamma_j)$.[12] This is confirmed as well by Eqs. (A2) and (A4) of the Appendix which, within the present approximation ($R_j, S_j \simeq 1/2$), reproduce exactly the equation $\dot{C}_{3j} = \{C_{3j}, H_{JJ}\}$ for the on-site charges C_{3j}. The special trait characterizing $\mathcal{H}$ is the quadratic term $A_{3j}B_{3j}$ that generates a coupled phase dynamics via Eqs. (14) and (15), namely, a linearized system of two U-coupled arrays. Also, this suggests to define here a quantity that describes the net local current between the two arrays. If we let A_j and B_j play the role of the Josephson wave functions, and A_{3j}, B_{3j} as on-site charges, such current turns out to satisfy the equation

$$I_j \simeq -\frac{T}{2}(\varphi_{j+1} - 2\varphi_j + \varphi_{j-1}), \tag{20}$$

where $I_j \doteq \dot{A}_{3j} - \dot{B}_{3j}$. Hence the tunneling phenomenon keeps track itself of the dependence on w, vanishing in the strong Coulomb repulsion regime ($U > 4T$).

IV. PHASE DYNAMICS

Apart from the case related to Eqs. (18) and (19), in the present paper we shall investigate solutions of Eqs. (8)–(11) such that only the phases play a relevant dynamical role, A_{3j} and B_{3j} being constant in time. If, on the one hand, the dynamical situations in which A_{3j}, B_{3j} are involved exhibit a complex behavior and their investigation goes beyond the purposes of the present paper, on the other hand, considering only α_j, β_j as dynamically active still entails situations that are far from being trivial and facilitates the recognition of the topological features that possibly characterize the solutions.

Hamiltonian (7) describes the dynamics of interacting classical angular momenta. The latter exhibits solutions that consistently match the semiclassical nature of the present approach the more, by appropriately changing the basis of canonical coordinates, one identifies some new variables that could assume macroscopically large values and exhaustively account for the system dynamics.[10] In general, for a given dynamical system, the excitations corresponding to the proper dynamical modes (if any) provide both the simplest and natural way to construct macroscopic semiclassical solutions. Unfortunately, the identification of proper modes is equivalent to making explicit solution of the Hamiltonian equations, which in our case are highly nonlinear. Nevertheless, based on the usual Fourier modes picture, where

$$C_j = L^{-1/2}\sum_{k=1}^{L} \exp(i\tilde{k}j)\tilde{C}_k,$$

with $\tilde{k} = 2\pi k/L$, $C = A, B$, one may wonder whether there exists any integrable case corresponding to associate the macroscopically large number of spin degrees of freedom with a finite number of excited Fourier modes. It turns out that this is the case, at least for two classes of solutions.

A. Vortex dynamics

First, it is easily verified that the case corresponding to two single excited Fourier modes p and q, one for each fluid, i.e., $\tilde{A}_p \doteq L^{1/2}R_A$, $\tilde{A}_k = 0$, $k \neq p$, and $\tilde{B}_q \doteq L^{1/2}R_B$, $\tilde{B}_k = 0$, $k \neq q$, is solution of Eqs. (8)–(11) with

$$A_j(t) = R_A \exp\{i[j\tilde{p} - \omega_A(p)t + \phi_A]\}, \tag{21}$$

$$B_j(t) = R_B \exp\{i[j\tilde{q} - \omega_B(q)t + \phi_B]\}, \tag{22}$$

where $R_C \equiv \sqrt{\frac{1}{4}-C^2}$ with $C=A,B$, and $A=A_3/L$, $B=B_3/L$, ϕ_A, ϕ_B are arbitrary phases accounting for the $U(1)$ symmetry of dynamical equations and

$$\omega_A(p)=(-\delta_A+UB)+4TA\cos\tilde{p}, \tag{23}$$

$$\omega_B(q)=(-\delta_B+UA)+4TB\cos\tilde{q}. \tag{24}$$

The corresponding energy per site is straightforwardly obtained as

$$E_{p,q}=U(A+\tfrac{1}{2})(B+\tfrac{1}{2})-2T[R_A^2\cos\tilde{p}+R_B^2\cos\tilde{q}]. \tag{25}$$

The main feature of solutions (21) and (22) is their topological character encoded by the winding numbers p and q. Notice that we have assumed periodic boundary conditions providing our 1D lattice with the topology of the circle, and A_j, B_j can be regarded as order parameters covering two $\mathbf{S}^1$ configuration spaces. Within this picture the indices p and q account for the number of times A_j and B_j cover their configurations spaces while j goes from 0 to L. Indeed such configurations are nothing but 1D vortex excitations once the phases of the order parameters are identified with the potential functions of two coupled fluids. Here the coupling is fully contained in the frequencies $\omega_A(p)$ and $\omega_B(q)$.

Interestingly, it is possible to evaluate explicitly correlation functions for solutions (21) and (22). Their physical meaning is better understood when writing them for the original fermionic system. In this case, two-site correlations within a single fluid (the one with up spins), read

$$\langle c_{j\uparrow}^{\dagger}c_{l\uparrow}+\text{H.c.}\rangle=2(2A)^{|l-j|-1}R_A\cos[\tilde{p}(j-l)],\quad l\neq j, \tag{26}$$

whereas for sites belonging to the two different fluids are

$$\begin{aligned}\langle c_{j\uparrow}^{\dagger}c_{l\downarrow}+\text{H.c.}\rangle=&\,2(2A)^{L-j}(2B)^{l-1}R_AR_B\\ &\times\cos\{j\tilde{p}-l\tilde{q}+[\omega_B(q)-\omega_A(p)]t\\ &+(\phi_A-\phi_B)\}.\end{aligned} \tag{27}$$

with $j\neq l$. As expected, in both cases long-range order does not emerge since $2|A|$, $2|B|$ are smaller than one in any nontrivial case. However, two remarkable features emerge. First, they manifestly keep track of the topological character of the solution through the winding numbers p and q. Second, but more important, the two-fluid correlation function also exhibits a time-dependent behavior, whenever the density of the two fluids or the topological charges are different. This last feature should be viable to experimental observation.

B. Staggered dynamics

The general class of solutions characterized by the phase dynamics is obtained when B_{3j}, A_{3j} are assumed to be assigned. In this case Eqs. (8)–(11) reduce to a linear system of equations for the variables A_j's, and B_j's where proper modes coincide with the eigenvalues of a certain secular equation. In fact, one should recall that assigning B_{3j}, A_{3j} and thereby reconstructing $|B_j|$, $|A_j|$, leaves the possibility to satisfy the eigenvalue problem by exploiting just the phases of B_j and A_j.

For A_{3j} and B_{3j} constant in time, Eqs. (10) and (11) are conveniently rewritten (see the Appendix) in terms of action-angle-like variables defined in Eq. (13), as

$$R_{j+1}\sin(\alpha_{j+1}-\alpha_j)+R_{j-1}\sin(\alpha_{j-1}-\alpha_j)=0, \tag{28}$$

$$S_{j+1}\sin(\beta_{j+1}-\beta_j)+S_{j-1}\sin(\beta_{j-1}-\beta_j)=0. \tag{29}$$

The general solution is not known. Of course a simple solvable case is obtained by assuming both R_j and S_j constant and independent of j. This leads to the vortex case discussed in the previous subsection. A further solution exhibiting an interesting dynamics is obtained by noticing that R_{j+1}, R_{j-1}, can be factored out from the above conditions upon assuming that $R_{2l}=R_E$ and $R_{2l+1}=R_O$, $\forall l$, with R_E, R_O fixed constants. The same assumptions can be implemented on S_{j+1}, S_{j-1}, so that when they are inserted in Eqs. (28) and (29), these turn out to depend only on the difference $\gamma_{j+1}-\gamma_j$, with $\gamma=\alpha,\beta$. The latter has two possible values satisfying the equations, γ_* or $\pi-\gamma_*$ for each j, with γ_* time-dependent function. Then Eqs. (8) and (9) can be solved explicitly, when rewriting them in the action-angle form of the Appendix. In fact, it turns out that a consistent solution is achieved provided $\gamma_{2j+1}-\gamma_{2j}\equiv\gamma_*$, and $\gamma_{2j}-\gamma_{2j-1}=\pi-\gamma_*$, for each j, which entails

$$\gamma_{2j+1}=j\pi+\gamma_1,\quad \gamma_{2j}=(j-1)\pi+\gamma_2. \tag{30}$$

γ_1 and γ_2 are time-dependent functions responsible for the system's phase dynamics as solutions of the corresponding equations given in Eqs. (A1) and (A3). For instance in the case $\gamma=\alpha$ they read

$$\begin{aligned}\alpha_1&=(\delta_A-UB_{3O})t+\alpha_1(0),\\ \alpha_2&=(\delta_A-UB_{3E})t+\alpha_2(0),\end{aligned} \tag{31}$$

while the analogue for β_1, β_2 is easily derived. Interestingly, the time-dependent part of the phases keeps track of the coupling between the two fluids for any nonvanishing value of the Coulomb repulsion U. Again, such a feature should be viable for experimental observation.

Apart from the initial conditions $\gamma_1(0)$, $\gamma_2(0)$, the solution (30), (31) clearly exhibits a staggering in the phases both on the even and on the odd sublattices. Making such a solution consistent with periodic boundary conditions constrains the length of the lattice L to be $L=4p$, $p\in\mathbf{N}$. Once more this feature can be related to the macroscopic excitation of some Fourier modes (two for each fluid). Explicitly for $C=A$

$$\begin{aligned}A_{L/4}&=\frac{1}{2}\sqrt{L}[R_E e^{i\alpha_2(0)}+iR_O e^{i\alpha_1(0)}],\\ A_{3L/4}&=\frac{1}{2}\sqrt{L}[R_E e^{i\alpha_2(0)}-iR_O e^{i\alpha_1(0)}],\end{aligned} \tag{32}$$

and $A_k=0$ for $k\neq p,3p$, the analogue holding as well for $C=B$, $\phi=\beta$.

The minimum energy per site E_s of the above staggered solution—to be compared with successive results for different phases—is found to be $E_s = U(\nu + |\nu|)/4$. It is important to observe how the independence of E_s from T (to be interpreted as the absence of a net global current) follows from the fact that the contributions to the hopping term coming from subsequent lattice bonds, let us say $(j, j+1)$ and $(j+1, j+2)$, cancel each other. At the microscopic level, however, the hopping terms actually contribute in terms of local currents (these are essentially given by $\gamma_{2j+1} - \gamma_{2j} = \gamma_*$, $\gamma_{2j} - \gamma_{2j-1} = \pi - \gamma_*$) with opposite sign.

C. Many-sublattices solution

Further solutions to Eqs. (8)–(11) that correspond to the excitation of a finite number of Fourier modes (endowed with a macroscopic character) can be recovered by partitioning first the lattice Λ into $n = L/q$ sublattices Λ_a of q sites (q divisor of L), and introducing then the collective variables

$$A_a \doteq \sum_{l=0}^{q-1} A_{ln+a}, \quad A_{3a} \doteq \sum_{l=0}^{q-1} A_{3(ln+a)}, \tag{33}$$

with $l \in (0, q-1)$, $a \in (1, n)$. Here A_a, A_a^*, and A_{3a} still fulfill the commutation relations of a (classical) algebra $su(2)$. It turns out that Eqs. (8)–(11) can be rewritten in terms of the above collective variables provided further assumptions are stated. These are $A_{3j} = A_{3a}/q$, $A_j = A_a/q$ with $j \in \Lambda_a$. When this is the case, dynamical equations reduce to a set of $4L/q$ equations now written in terms of A_{3a}, A_a, B_{3a}, B_a exhibiting the same structure. In the Fourier transformed space this amounts to the excitations of n modes, i.e.,

$$\tilde{A}_k = \frac{1}{\sqrt{N}} \sum_{a=1}^{n} e^{i\tilde{k}a} A_a, \quad \tilde{A}_l = 0, \tag{34}$$

($\tilde{k} = 2\pi k/N$) for $k = mq$, $l \neq mq$ $(0 < m \leqslant n)$, respectively. Solutions within this class are now obtained by solving the remaining $4n$ equations, which preserve the same complex structure of the original ones.

For the simplest case $n = 2$ ($n = 1$ being a subclass of vortexlike solutions) the dynamical equations are represented by

$$i\dot{A}_1 = (-\delta_A + UB_{31})A_1 + 4TA_{31}A_2, \tag{35}$$

$$i\dot{B}_1 = (-\delta_B + UA_{31})B_1 + 4TB_{31}B_2, \tag{36}$$

$$i\dot{A}_2 = (-\delta_A + UB_{32})A_2 + 4TA_{32}A_1, \tag{37}$$

$$i\dot{B}_2 = (-\delta_B + UA_{32})B_2 + 4TB_{32}B_1. \tag{38}$$

together with those for A_j^* and B_j^*. Correspondingly Hamiltonian (7) takes the form

$$H_2 = \frac{N_s}{2}\Big\{ U/2 - \sum_{C=A,B} [\delta_C(C_{31} + C_{32}) - \nu_C] + U(A_{31}B_{31} + A_{32}B_{32}) - 2T(A_1A_2^* + B_1B_2^* + \text{c.c.}) \Big\}. \tag{39}$$

As the number of first integrals of motions is 3 (H, A_3, and B_3), whereas the equations are now 8, this case is nonintegrable. However, being interested in phase dynamics in which case A_{3j} and B_{3j} are constants for each j, the solution to Eqs. (35)–(38) can be worked out explicitly. The latter is characterized by collective frequencies λ_A, λ_B for the A_j's and B_j's of the form $C_j = C_j(0)\exp(i\lambda_C t)$ $(C = A, B,\ j = 1, 2)$, which are independent from each other.

It is important to notice how the case presently studied differs from the staggered solutions described above since $C_{j+2} = C_j$ is not contained in Eqs. (28)–(29), namely, $\text{Im}[C_j^*(C_{j+1} + C_{j-1})] = 0$. When $C_j(t)$ are inserted in Eqs. (35)–(38) one is able to recast them in the form

$$U(B_{31} - B_{32}) = 4T\left(A_{32}\frac{A_1}{A_2} - A_{31}\frac{A_2}{A_1}\right), \tag{40}$$

$$U(A_{31} - A_{32}) = 4T\left(B_{32}\frac{B_1}{B_2} - B_{31}\frac{B_2}{B_1}\right), \tag{41}$$

$$2\delta_A - \lambda_A = U\nu_B + 4T\left(A_{32}\frac{A_1}{A_2} + A_{31}\frac{A_2}{A_1}\right), \tag{42}$$

$$2\delta_B - \lambda_B = U\nu_A + 4T\left(B_{32}\frac{B_1}{B_2} + B_{31}\frac{B_2}{B_1}\right), \tag{43}$$

where C_j (C_{3j}) stay for initial conditions $C_j(0)$ $[C_{3j}(0)]$, and the constant of motion

$$\nu_A \equiv A_{31} + A_{32}, \ \nu_B \equiv B_{31} + B_{32} \tag{44}$$

are input data, whereas δ_A, δ_B, A_{3j}, B_{3j} (consistently with $\nu_A, \nu_B = \text{const}$) are the unknown parameters to be fixed.

It is worth noticing that Eqs. (40) and (41) turn out to be completely independent from λ_A, λ_B while in Eqs. (42) and (43) λ_A and λ_B can be incorporated inside δ_A and δ_B by redefining them as $\Delta_C = \delta_C - \lambda_C/2$, $C = A, B$. At the operative level this fact allows one to reconstruct the solution of Eqs. (40)–(43) for $\lambda_C \neq 0$ from the case $\lambda_C = 0$, which by the way identifies the fixed points of Eqs. (35)–(38). The investigation of such points is deepened in the next section.

V. FIXED POINTS OF TWO-SUBLATTICE SOLUTION

The present approach is able to give a (simplified) description of the system dynamics, with a number of interesting features, as we have seen in the previous section. Nevertheless, as a secondary effect, it also gives the system equilibrium states, which coincide in fact with fixed points of the equations of motion. Many other (mean-field-like) approaches are focused on the study of equilibrium and especially ground states of Hamiltonian (7). For instance, from the Hartee-Fock approximation[13] it is known that the $T = 0$ phase space contains an antiferromagnetic, a ferromagnetic, and a paramagnetic phase for $U > 0$. In this section we shall see that a similar description of the ground-state phase can be already obtained by studying fixed points of the simple two-sublattice solution, the latter being given by Eqs. (40)–(43) for $\lambda_C = 0$.

In particular, as Eqs. (42) and (43) just fix δ_A, δ_B, we search for the solutions of Eqs. (40) and (41), in which the unknowns are two. It is convenient to introduce the pair of

new variables $a=A_{31}A_{32}$, $b=B_{31}B_{32}$, in terms of which the above equations reduce to the pair of fourth order, coupled equations

$$(\nu_B^2-4b)=g^2\frac{(1+4a)^2(\nu_A^2-4a)}{(1+4a)^2-4\nu_A^2}, \tag{45}$$

$$(\nu_A^2-4a)=g^2\frac{(1+4b)^2(\nu_B^2-4b)}{(1+4b)^2-4\nu_B^2}, \tag{46}$$

with $g=4T/U$. The two equations (45) and (46) can be recast into a single eight-degree equation for the variable a,

$$[Z^2(1-g^4)-4\nu_A^2][(1+\nu_B^2)(Z^2-4\nu_A^2)-g^2Z^2(\nu_A^2+1-Z)]^2=4\nu_B^2(Z^2-4\nu_A^2)^3, \tag{47}$$

where $Z\doteq 1+4a$, and the factor ν_A^2-4a, which provides an independent solution, has been factored out [see (i) below]. The variable b is then easily worked out from Eq. (45).

First, let us notice that the independent solution $\nu_A^2-4a=0$ implies $\nu_B^2-4b=0$ leading to $a=\nu_A^2/4$, $b=\nu_B^2/4$. As $\nu=\nu_A+\nu_B=2(s_a\sqrt{a}+s_b\sqrt{b})$ with $s_a=\pm 1$, $s_b=\pm 1$, this solution implies $A_{31}=A_{32}=\nu_A/2$, $B_{31}=B_{32}=\nu_B/2$ (two-sublattice solutions with ferromagneticlike order on each sublattice). It has energy

$$2\frac{H}{N_s}=\frac{U}{2}\left[1+\nu+\nu_A\nu_B+\frac{g}{2}(\nu_A^2+\nu_B^2-2)\right], \tag{48}$$

which matches the one of vortex solution $E_{p,q}$ [see Eq. (25)] in the untwisted case $p=q=0$. For fixed filling $\nu=\nu_A+\nu_B$ its minimum value depends on the actual value of p. When $g<1$ (i.e., $U>4$, this is reached either for $\nu_A=\nu$, $\nu_B=0$ or for $\nu_B=\nu$, $\nu_A=0$, in which case the energy becomes

$$E_{pf}=\frac{U}{2}\left(1+\nu-g+\frac{g}{2}\nu^2\right), \tag{49}$$

the solution describing ferromagnetism away from half-filling within a single cluster, in that the average magnetization on the cluster $M=(\nu_A-\nu_B)/2$ coincides with $\pm\nu/4$. The subindex p in E_{pf} is to remind us that the solution on the lattice, due to the arbitrary choice of the sign of M on each cluster, does *not* exhibit ferromagnetic order.

On the contrary, for $g>1$ the minimum value of expression (48) is reached when $\nu_A=\nu_B=\nu/2$. Physically, it corresponds to a paramagnetic solution even within a single cluster, and has energy

$$E_p=\frac{U}{2}\left[\left(1+\frac{\nu}{2}\right)^2-g\left(1-\frac{\nu^2}{4}\right)\right]. \tag{50}$$

Having in mind the phase diagram known from mean-field-like Hartree-Fock treatment of the Hubbard model, an antiferromagnetic solution is also expected, where the energy should be lower than both E_f and E_p near half-filling and for large U. This can be worked out as a solution of Eq. (47) when the magnetization is zero, namely $\nu_A=\nu_B$. In this case, it is easily realized that Eq. (47) can be rewritten as the product of a second-order factor $(g^2-1)Z^2+4\nu^2$ (real for $g<1$) and a sixth-order factor which, in the range of parameters physically allowed, never provides real solutions. On the contrary, the vanishing of the second-order factor in a, in fact, leads to an antiferromagnetic solution. This can be seen by first realizing that an analogous equation holds also for b, so that finally Eqs. (45) and (46) reduce to two second order ones

$$1=\frac{g^2(1+4a)^2}{(1+4a)^2-4\nu_A^2}, \tag{51}$$

$$1=\frac{g^2(1+4b)^2}{(1+4b)^2-4\nu_B^2}, \tag{52}$$

which in order to consistently match $\nu_A\equiv\nu_B$ imply $a=b$, with

$$b=a=\frac{1}{4}\left(\frac{2|\nu_A|}{\sqrt{1-g^2}}-1\right). \tag{53}$$

Notice that, away from half-filling (which corresponds to $\nu_A=\nu_B=0$), the condition $g<1$ follows from Eqs. (51) and (52). Moreover, when calculating explicitly A_{31} ($A_{32}=\nu_A-A_{32}$) and B_{31} ($B_{32}=\nu_B-B_{32}$) through formula (24), which reads

$$A_{31}\equiv\frac{1}{2}\left(\nu_A\pm\sqrt{\nu_A^2+1-2\frac{|\nu_A|}{\sqrt{1-g^2}}}\right), \tag{54}$$

$$B_{31}\equiv\frac{1}{2}\left(\nu_B\pm\sqrt{\nu_B^2+1-2\frac{|\nu_B|}{\sqrt{1-g^2}}}\right), \tag{55}$$

one singles out the further restriction $|\nu_A|=|\nu_B|<\sqrt{(1-g)/(1+g)}$. The apparent freedom in choosing the sign in Eqs. (54) and (55) just corresponds to exchange the role of A_{31} and A_{32} (B_{31} and B_{32}). In fact, the physical solutions turn out to be just two, in that the condition $a=b$ can be implemented in two different ways, namely $A_{31}=B_{31}$, $A_{32}=B_{32}$ (paramagnetic), and $A_{31}=B_{32}$, $A_{32}=B_{31}$ (antiferromagnetic). The energies corresponding to such solutions,

$$E_p'=\frac{U}{2}(1+\nu)+U(A_{31}^2+A_{32}^2)-8T\sqrt{\frac{1}{4}-A_{31}^2}\sqrt{\frac{1}{4}-A_{32}^2},$$

$$E_{af}=\frac{U}{2}(1+\nu)+2UA_{31}A_{32}-8T\sqrt{\frac{1}{4}-A_{31}^2}\sqrt{\frac{1}{4}-A_{32}^2},$$

differ only due to the U term, which is manifestly lower in the antiferromagnetic case. It turns out that the antiferromagnetic cluster energy

$$E_{af}=\frac{U}{2}(\nu+|\nu|\sqrt{1-g^2}) \tag{56}$$

is always lower than paramagnetic case within the domain specified by $|\nu_A|=|\nu_B|<\sqrt{(1-g)/(1+g)}$.

The successive comparison among Eqs. (50), (49), and (56) shows that the ground-state phase space for this two-sublattices solution (Fig. 1) exhibits a structure in qualitative agreement with many other theories, in particular, the one

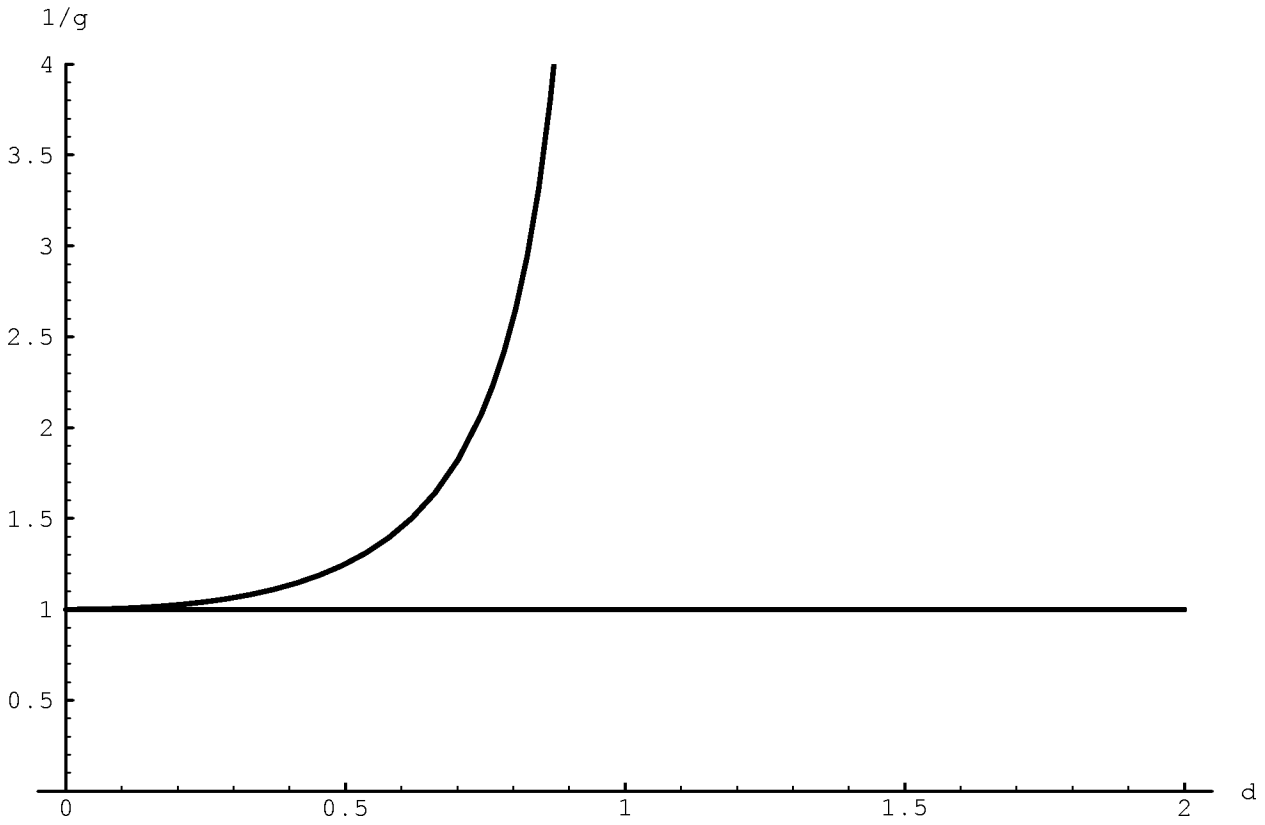

FIG. 1. The ground-state phase diagram of the one-band model for the two-site solution: $d=\nu$ is the electron doping ($d=0$ half-filling) on the two-site cluster, and $1/g=U/4T$. Its structure is in qualitative agreement with the diagram of Ref. 10, p. 256.

obtained in the low-density approximation for the one-band model (Ref. 10). Moving from half-filling, in which case a magnetic phase is found for $U>4T$, the antiferromagnetic phase takes place at increasing values of U, and in any case, for filling greater than one quarter. Indeed, by requiring that $E_{af}<E_{pf}$, the transition line to the antiferromagnetic phase is given by

$$\nu=\frac{1}{g}(g-1+\sqrt{1-g^2})>0. \tag{57}$$

For lower values of filling, the system is a nonmagnetic metal. Within such regime an extra transition emerges for $g=1$ from a paramagnetic solution with ferromagnetic structure on each cluster (energy E_{pf}), and a paramagnetic solution with no order even within the clusters (energy E_p). Apparently by increasing U the lattice begins to organize towards ferromagnetism. Let us notice that, consistently with the 1D character of the model studied, both ferromagnetic and antiferromagnetic solutions exhibit only local order, in that the actual value of the magnetization on different two-site clusters is uncorrelated.

In the previous section we explicitly gave the energies corresponding to some simple solutions of the equation of motions exhibiting nontrivial dynamics. A natural question is then whether some of these solutions survive down to the ground state, or not. Interestingly, one can verify that, in fact, the staggered solution, with energy E_s, at half-filling turns out to be degenerate with the two-site antiferromagnetic solution described above, with energy E_{af}. Indeed, both of them in this case have a vanishing hopping term, in agreement with the expected insulating behavior of such regime, and in practice on the single cluster the two solutions coincide. However, the explicit solution of the equations of motion in the staggered case proves that at a dynamical level the only consistent way of moving from the fixed point is by means of the staggered choice of phases.

VI. CONCLUSIONS

The main object of this paper has been to develop an approach to the Hubbard model quantum dynamics that is not based on the particular physical regime under investigation, on the one hand, and is capable of reformulating the model dynamics in a form more tractable than that relying on the direct diagonalization of the model Hamiltonian, on the other. Such requirements have been achieved by combining three ingredients, which are the representation of quantum dynamics within a coherent-state picture, the expression of the Hubbard Hamiltonian in terms of spin variable (2) issued from its fermionic standard form through the Jordan-Wigner transformation (1), and the implementation of the TDVP method. The choice of the trial state (6) has generated Hamiltonian (7) (that is $\mathcal{H}$ with the constraints $\chi_C=0$, $C=A, B$) whose dynamics is governed by Eqs. (8) and (11), and accounts for the evolution of the spin operator expectation values.

The resulting dynamical scenery has revealed both a rich structure—that corresponding to a pair of XX models coupled through the Coulomb term—and interesting links with other models.

For $|A_j|^2, |B_j|^2 \simeq 0$, one obtains a model of two coupled

fluids at low density. In particular, in this limit, the dynamics has been recognized to have the form of two coupled lattice NLSE. A feature that is unusual for the standard NLSE comes from the dependence of the off-site terms in Eqs. (8) and (9) on the signs of C_{3j}, which allows for the fragmentation of the planar lattice in regions where either $C_{3j} \simeq +1/2$ (sites occupied by electrons of type C), or $C_{3j} \simeq -1/2$ (local depletion of electrons of type C). The latter case suggests the occurrence of solitonlike behavior in correspondence to the negative sign of the off-site terms.

The opposite regime $|A_j|^2, |B_j|^2 \simeq 1/4$ has been studied in Sec. III, where the equations of motion have revealed that the model actually describes two coupled Josephson-junction arrays. In particular the condition $|C_j|^2 \simeq 1/4$ makes emerge a dynamics concerning essentially the phases α_j, β_j that can be solved exactly after reducing the equations of the Appendix to the linear system described by Eqs. (14) and (15). Its main feature is certainly the macroscopic effect of phase locking $[(\alpha_j - \beta_j) \to 0]$ which is enacted when going from $U<4T$ to $U>4T$, and might be related to the metal-insulator transition exhibited by the Hubbard model.

Pursuing the investigation of dynamical situations in which phases are active and $|A_j|^2, |B_j|^2 = \text{const}$ has led us to recognize two other interesting results. First, a set of topological solutions has been obtained by considering uniform configurations $C_{3j} = C_3/L$, $C = A,B$, which are nontrivial when one excludes the half-filling case. The phases α_j and β_j are allowed to change as j is varied so as to give rise to a pair of vortexlike configurations labeled by two integers p and q for A_j and B_j (the fluid order parameters), respectively. Also, the time behavior exhibits a dependence on the electronic fillings as well as on the topological characters through the frequencies $\omega_A(p)$ and $\omega_B(q)$.

A second class of solutions has been obtained instead when considering the solutions of Eqs. (8) and (9) fulfilling the constraints $C_{3j} = \text{const}$ at each site, and depending on a unique frequency. Despite the strong simplification thus introduced, the complexity of the problem is still dramatic as shown by the dynamical constraints (28) and (29). It is worth recalling that their implementation corresponds to find first the eigenvalues of Eqs. (8) and (9) in which C_{3j} are regarded as constant, assigned parameters, and singling out then the subset of eigenvectors such that $|C_j|$ are compatible with the assigned C_{3j}. The staggered solutions [see (31) and (32)] represent the case where the avalanche of initial conditions is reduced to a set of four data, namely the values of $|C_j|$ for the sublattices of both even and odd sites.

Based on the polygonal symmetry of the spin equations of motion their number has been reduced by introducing the collective variables (33) in Sec. III C. The first nontrivial case (but also the only one directly tractable in an analytic way) has been shown to correspond to the two-sublattice solutions ($C_j = C_l$, $C_{3j} = C_{3l}$, $l = j+2$, $\forall j$). The analysis of the fixed points of Eqs. (35)–(38) allows one to reconstruct the set of configurations in which those corresponding to the minimum energy are implicitly contained as a consequence of the absence of dynamics. In Sec. V we specialized to the latter in order to obtain a zero-temperature phase space. Noticeably, we have seen that already such a simple two-sublattice solution contains all the qualitative features of similar diagrams obtained in many other theories. Hence, we argue that the general solution of fixed-point equations, if avaliable on finite lattices by means of numerical analysis, should exhibit a richer structure than the one obtained within standard mean-field schemes even for what concerns the zero-temperature phase space.

Further developments of the present work can be envisaged along the following lines. As to the transformation (1) it is important to notice how its use has been possible because of the 1D character of the system. In higher dimensions, in fact, this transformation depends explicitly on the 1D path employed to cover and thus enumerate exhaustively the lattice sites. Such a dependence introduces in the hopping term of the Hamiltonian a site-dependent exponential phase factor, which does not prevent the implementation of the approach developed here. Hence, in spite of the increased complexity thus introduced, a natural extension of the present work is in the analysis of the 2D case dynamics.

As a matter of fact, due to the large number of degrees of freedom involved, the 1D case itself is already not fully tractable via numerical investigations. In this respect, focusing on zero-dimensional systems is almost expected in order to have a dependable numerical description. On the other hand, it is well known that the physics of such mesoscopic systems (e.g. quantum dots and Josephson junctions) is properly depicted in many cases by Hubbard-like Hamiltonians.[14,15] Further investigation of such systems within the scheme proposed here seems promising.

A final point still deserves to be deepened, which is the requantization of the spin variables. Despite the obvious difficulty of such a task in general,[6] the dynamical situations here investigated, involving the macroscopic excitation of few system modes, seems quite feasible to this end.

ACKNOWLEDGMENTS

Part of this work was performed while the authors were visiting the Department of Mathematics of the Open University (U.K.). The authors would like to thank Professor A. Solomon for stimulating discussions. One of them (V.P.) is grateful to the Open University for its hospitality and for supporting his visit. The INFM is also acknowledged for financial support.

APPENDIX

After setting $A_j = R_j \exp(i\alpha_j)$, $B_j = S_j \exp i\beta_j)$, where $R_j \equiv (1/4 - A_{3j}^2)^{1/2}$, $S_j \equiv (1/4 - B_{3j}^2)^{1/2}$ with the Poisson brackets $\{\alpha_l, A_{3j}\} = \delta_{l,j}/i\hbar$, $\{\beta_l, B_{3j}\} = \delta_{l,j}/i\hbar$, it is found

$$\dot{\alpha}_j = \delta_A - UB_{3j} + 2TA_{3j} \sum_{i \in (j)} \frac{R_i}{R_j} \cos(\alpha_i - \alpha_j), \quad \text{(A1)}$$

$$\dot{A}_{3j} = 2TR_j \sum_{i \in (j)} R_i \sin(\alpha_j - \alpha_i), \quad \text{(A2)}$$

$$\dot{\beta}_j = \delta_B - UA_{3j} + 2TB_{3j} \sum_{i \in (j)} \frac{S_i}{S_j} \cos(\beta_i - \beta_j), \quad \text{(A3)}$$

$$\dot{B}_{3j} = 2TS_j \sum_{i \in (j)} S_i \sin(\beta_j - \beta_i), \quad \text{(A4)}$$

where (j) indicates the set of the nearest-neighbor sites.

[1] W. M. Zhang, D. H. Feng, and R. Gilmore, Rev. Mod. Phys. **62**, 867 (1990).
[2] A. K. Kerman and S. E. Koonin, Ann. Phys. (N.Y.) **100**, 332 (1976).
[3] A. G. Basile and V. Eltser, Phys. Rev. E **51**, 5688 (1995).
[4] A. Montorsi and V. Penna, Phys. Rev. B **55**, 8226 (1997).
[5] E. H. Lieb, Commun. Math. Phys. **31**, 327 (1973).
[6] T. Fukui and Y. Tsue, Prog. Theor. Phys. **87**, 627 (1992); A. Inomata, H. Kuratsuji, and C. C. Gerry, *Path Integral and Coherent States of SU(2) and SU(1,1)* (World Scientific, Singapore, 1992).
[7] B. S. Shastry, Phys. Rev. Lett. **56**, 1529 (1986).
[8] S. Flach and C. R. Willis, Phys. Rep. **5**, 181 (1998).
[9] See, A. L. Fetter, cond-mat/9811366 (unpublished).
[10] D. C. Mattis, *The Theory of Magnetism: Statics and Dynamics* (Springer-Verlag, Berlin, 1981).
[11] D. R. Tilley and J. Tilley, *Superfluidity and Superconductivity* (Hilger, Bristol, 1986).
[12] Quantum effects in Josephson-junction arrays are reviewed in the *Proceedings of the ICTP Workshop on Josephson Junction Arrays*, edited by H. A. Cerdeira and S. R. Shenoy [Physica B **222**, 336 (1996)].
[13] J. E. Hirsch, Phys. Rev. B **31**, 4403 (1985).
[14] M. Rontani, F. Rossi, F. Manghi, and E. Molinari, Appl. Phys. Lett. **72**, 957 (1998).
[15] L. Jacak, P. Hawrylak, and A. Wojs, *Quantum Dots* (Springer-Verlag, Berlin, 1998); J. Yngvason, math-ph/9812009 (unpublished).